Table 1 Overview of HSAN disease-causing genes, inheritance pattern, and cardinal phenotypic features

Gene symbol	HSAN type	Inh	Onset age	Cardinal clinical features
SPTLC1	IA	AD	Adulthood	Loss of pain and temperature sensation; occasional autonomic involvement; variable sensorineural deafness and distal motor involvement[1,2]
SPTLC2	IC	AD		
ATL1	ID	AD	Early adulthood	Severe loss of pain, temperature, and vibration sensation; ulcero-mutilation; spastic paraparesis; rare autonomic involvement[3]
DNMT1	IE	AD	Childhood-adulthood	Severe sensory loss; ulcero-mutilation; sensorineural hearing loss; early-onset dementia; no autonomic symptoms[4-6]
WNK1	IIA	AR	Congenital—early childhood	Severe distal loss of touch, pain, and temperature sensation; mutilations in hands and feet; mild or asymptomatic autonomic dysfunction[7,8]
FAM134B	IIB	AR	Childhood	Severe loss of pain and temperature sensation; ulcero-mutilation; autonomic dysfunctions[9]
KIF1A	IIC	AR	Childhood	Severe loss of pain, temperature, vibration, and position sensation; ulcero-mutilation; distal muscle weakness; developmental delay and short stature[10]
IKBKAP	III	AR	Congenital	Familial dysautonomia; gastrointestinal and respiratory dysfunction; scoliosis; relative indifference to pain and temperature[11-13]
NTRK1	IV	AR	Congenital—early childhood	Loss of pain and temperature sensation; anhidrosis; episodic fever; mild mental retardation; joint deformities[14]
NGF	V	AR	Congenital—adulthood	Reduced sensation of pain and temperature; variable autonomic dysfunctions; painless fractures; joint deformities; mild mental retardation[15,16]
DST	VI	AR	Congenital	Dysautonomia; hypotonia; facial deformity; decreased pain response; joint contractures; retardation; respiratory failure; early death[17]

Abbreviations: AD = autosomal dominant; AR = autosomal recessive; *ATL1* = atlastin GTPase 1; *DNMT1* = DNA (cytosine-5)-methyltransferase 1; *DST* = dystonin; *FAM134B* = family with sequence similarity 134, member B; *IKBKAP* = inhibitor of κ light polypeptide gene enhancer in B cells, kinase complex-associated protein; Inh = inheritance; *KIF1A* = kinesin family member 1A; *NGF* = nerve growth factor (β polypeptide); *NTRK1* = neurotrophic tyrosine kinase, receptor, type 1; *SPTLC1* = serine palmitoyltransferase, long chain base subunit 1; *SPTLC2* = serine palmitoyltransferase, long chain base subunit 2; *WNK1* = WNK lysine deficient protein kinase 1.

In this study, using a next-generation sequencer, in 9 Japanese patients who were diagnosed with HSAN based on their clinical, in vivo electrophysiologic, and pathologic features, 11 known HSAN disease–causing genes and 5 related genes including *SCN9A* were screened. We identified a homozygous frameshift mutation in *SCN9A* of 2 patients/families. Therefore, we demonstrate that loss-of-function *SCN9A* mutation can produce a typical HSAN phenotype, and we propose this new classification as HSAN type IID. This study also broadened the spectrum of clinical phenotypes in patients with *SCN9A*-related disorders. Furthermore, on the basis of clinical, in vivo electrophysiologic, and pathologic findings, we attempted to elucidate the pathogenesis of the mutated $Na_V1.7$.

METHODS All patients who were referred to our department from 2000 to 2012 and who had sensory and autonomic nerve dysfunctions were selected. After excluding patients who had associated multiple motor nerve involvement, 9 patients were enrolled and genotyped in this study. Besides the 11 known HSAN disease-causing genes described above, we also investigated another 5 genes that might also cause sensory and autonomic symptoms, including *SCN9A*, *CCT5*, *PRNP*, *FLVCR1*, and *RNF170*.

The protocol of the following study was reviewed and approved by the Institutional Review Board of Kagoshima University. All patients and family members provided written informed consent to participate in this study.

Pathologic study. Sural nerve biopsies, performed at the age of 42 years in patient 1 and at the age of 25 years in patient 2, were analyzed according to standard morphologic procedures for light and electron microscopy.[18] A portion of the specimen was prepared for teased fiber analysis and classified according to Dyck's criteria.[19] The diameter and density of the myelinated fibers were analyzed with a Luzex AP image analyzer (Nireco Corporation, Tokyo, Japan).

Mutation sequencing. Genomic DNA was extracted from the peripheral blood leukocytes.

Using the Primer 3 program, we designed 375 oligonucleotide primers that covered all 357 coding exons and exon-intron junctions with amplicon lengths of 400–500 base pairs. Briefly, all target fragments of 9 patients were amplified by multiplex PCR (QIAGEN Multiplex PCR Kit; QIAGEN GmbH, Hilden, Germany) and ligated with specified indexes, respectively, then screened on the MiSeq sequencing system simultaneously in

accordance with the manufacturer's protocol. The results were mapped to the genome reference sequence in the CLC Genomics Workbench 4 (CLC Bio, Aarhus, Denmark) and then analyzed with tablet software.[30]

The polymorphic and pathogenic natures of the confirmed variants were checked against the single nucleotide polymorphism database (dbSNP) (http://www.ncbi.nlm.nih.gov/snp/) and the 1000 Genomes database (http://browser.1000genomes.org/index.html). To confirm the suspected pathogenic mutations or low coverage domains (depth less than 10) in the MiSeq sequencing output, Sanger sequencing was also performed using the same methodology as the one employed in a previous study.[31] We screened 100 Japanese population control patients for the c.3993delGinsTT mutation.

RESULTS **Patients.** ***Patient 1.*** This 50-year-old man was the sixth child from a consanguineous family. No abnormalities were noted at birth or in the early developmental stages except for slight hyposmia since childhood. Since primary school, pain perception started to decrease in his hands and feet. At 30 years of age, he underwent lumbar spinal fixation, but felt no pain. After 40 years of age, the numbness progressed from the distal to the proximal limbs. Furthermore, his toes could not perceive temperature well when he entered his bath, and while walking, his right slipper always slipped off. There was no history of episodes of unexplained vomiting or dysphagia. A detailed physical examination revealed multiple skin lesions, including a burn mark on the right middle finger, which was caused by a cigarette. No pupillary abnormalities were observed. His muscle strength was normal, except grade 4+/5 weakness in the right tibialis anterior muscle. He also had a slight steppage gait. All reflexes were diminished, and his pathologic reflexes were negative. Pain and temperature perception were reduced in the distal limbs and absent in his feet. However, sense of vibration, joint position, and pressure were all preserved. Postural hypotension was excluded. During the sweating test, no sweating was observed in his face or any of his limbs, except in the palm of his left hand. Asymptomatic sensorineural hearing loss with an increase in the 4,000-Hz threshold in the left ear was diagnosed by an otorhinolaryngologist. MRI of the brain was normal.

In nerve conduction study, all motor nerve conduction velocity and compound muscle action potentials (CMAP) values were normal, except for a slightly reduced CMAP in the right tibial nerve at 3.5 mV (normal range, >4.4 mV). Sensory nerve conduction velocity (SCV) was slightly slow in the right median and ulnar nerve at 45.2 m/s (normal range, >47.2 m/s) and 40 m/s (normal range, >46.9 m/s), respectively, and moderately slow in the right sural nerve at 27.5 m/s (normal range, >40.8 m/s). SNAP amplitudes were markedly reduced in the right median nerve (0.9 μV; normal range, >7.0 μV), bilateral ulnar nerves (1.3 and 2.2 μV; normal range, >6.9 μV), and the right sural nerves (1.0 μV; normal range, >5.0 μV). However, the SCV and SNAP in the left median nerve were normal.

Patient 2. This 33-year-old man was from a nonconsanguineous family having no history of neurologic

Figure 1 **Clinical pictures of patient 2**

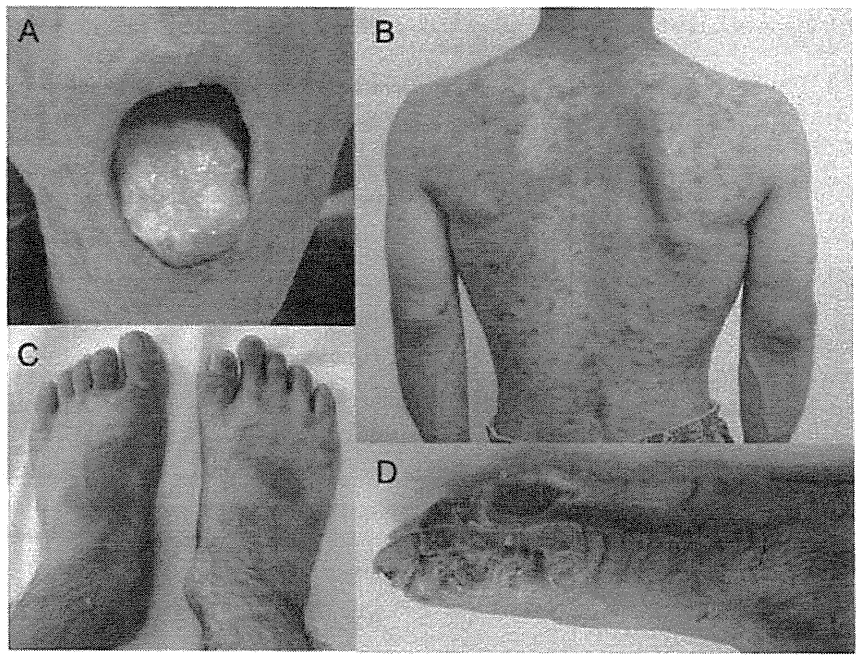

(A) Reduced number of fungiform papilla on the tongue. (B) The back of patient 2, showing scattered rash, pigmentation, and short humerus. (C) Short right hallux. (D) Multiple painless ulcers and deformed joints in the fingers.

disorders. Decreased pain and temperature perception was noted at birth. When he was a year old, his feet were burnt after he walked on asphalt on a hot summer day, and this eventually progressed to osteomyelitis. Subsequently, he underwent operations of the right tibia and both feet, but he could not feel any pain. Before enrolling in primary school, hearing loss in the left ear and hyposmia were detected. He experienced occasional urinary and fecal incontinence, and frequent urination at night. His height was 157 cm, and he had a short humerus (27.5 cm) and right hallux (figure 1, B and C). Left acetabular dysplasia was noticed, which contributed to his left lower limb being 3 cm longer than his right lower limb. Rash and pigmentation were scattered over his chest and back (figure 1B), and several painless ulcers and deformed joints were observed in his fingers (figure 1D). Tendon hyperreflexia was noted in the lower limbs, and pathologic reflexes were negative. Pain perception was impaired in a glove–stocking pattern. Sense of vibration, joint position, and pressure were all normal. The sweating test revealed reduced sweating tendency throughout the body and especially in the trunk, except for his hands and feet. Postural hypotension was excluded, and brain MRI was normal. A lacrimal secretion anomaly was also detected. Otorhinolaryngologic examinations revealed the following: deafness in the left ear and minimal hearing loss in the right ear, glossopharyngeal and chorda tympani nerve abnormalities in the gustatory sensation test, reduced number of fungiform papilla on his tongue (figure 1A), and a decline in olfactory acuity as tested by a jet stream olfactometer. Examinations of the urinary tract excluded any organic disease.

The nerve conduction study revealed all motor nerve conduction velocity and CMAP values within normal ranges. The SCV was slightly slow in the right median and ulnar nerves (45.2 m/s and 46.2 m/s, respectively). However, SNAP was moderately decreased in the bilateral median (7 and 5.7 μV) and ulnar (3.3 and 4.4 μV) nerves. Nevertheless, no abnormalities were detected in sural nerve SCV and SNAP values.

Patient 3. This 55-year-old woman was an elder sister of patient 1. Her pregnancy was uneventful and delivery was normal. She had recurrent fractures and underwent operations for the left thigh (at age of 3 years and 8 years), right thigh (at age 11 years), and left elbow (primary school). When she was 30 years old, she perceived no pain after her feet were burnt on a heater. Anhidrosis was also noted, but after the age of 45 years, occasional sweat was secreted on her back. There was no evident hyposmia or hearing loss. At present, she is able to stand up and walk using

Figure 2 Clinical courses of the 3 patients

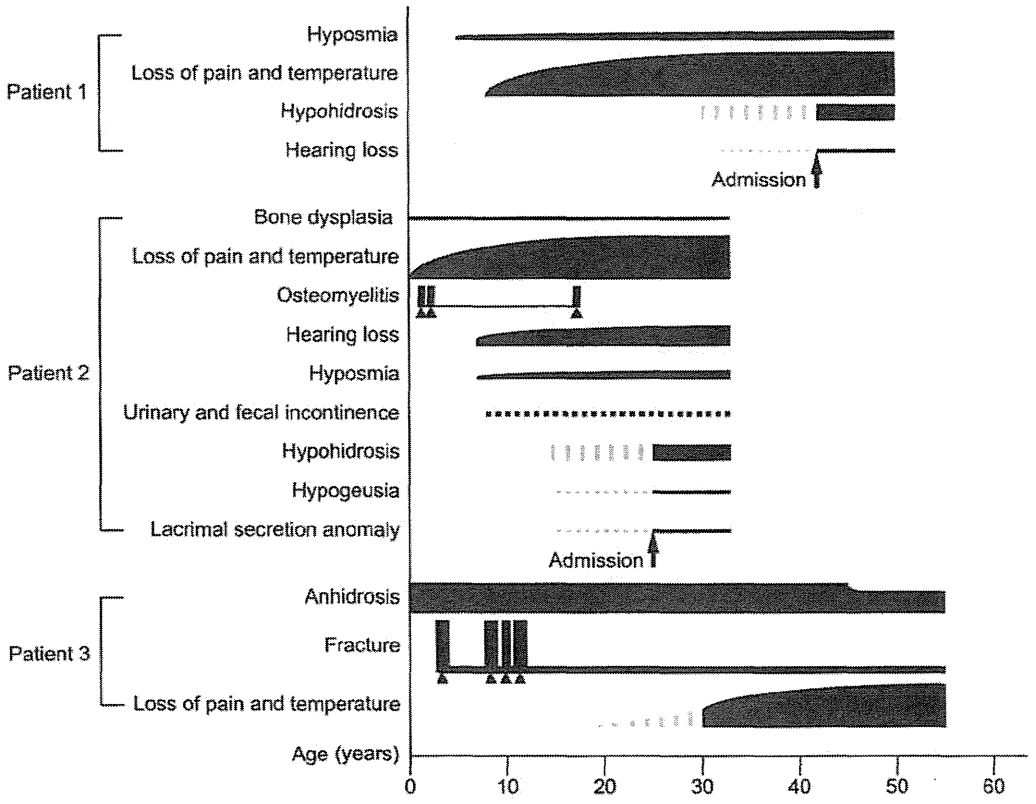

The solid triangles (▲) indicate surgery.

her hands for support. Cranial nerve examinations were normal. Deformities of the left elbow, right foot, and bilateral lower limbs were noted. Muscle strength testing was normal in the upper limbs, whereas the strength in the lower limb muscles decreased to grades 2/5–4/5. Pain and temperature perceptions were reduced in the distal lower limbs and the anterior part of the right thigh, which may have been involved because of damage from surgery. The sense of vibration and joint position were preserved. Reflexes in her lower limbs were absent, and her pathologic reflexes were negative. Osteoporosis was excluded by an orthopedist.

The clinical courses of the 3 patients described above, including the onset and imaged severities of each symptom, are shown in figure 2.

Pathologic studies. In patient 1, the number of myelinated fibers was markedly decreased in all fasciculi, but the changes varied in their scale and extent. A histogram of the fiber diameter indicated a marked loss of large myelinated fibers relative to small myelinated fibers. Some remaining myelinated fibers had thinner myelin sheaths and some exhibited axonal degeneration. An electron microscopic study revealed clusters of Schwann cell processes, which may have been caused by the axonal degeneration of unmyelinated fibers (figure 3A). Contrary to the findings in patient 1, the number of myelinated fibers in patient 2 was slightly decreased, even with marked clinical symptoms. The histogram of fiber diameter showed a normal pattern. Electron microscopy showed that unmyelinated fibers were fairly preserved (figure 3B). No demyelinated fibers or inflammatory cells could be found in either patient.

Genetic studies. Using the MiSeq sequencing system, all of the 9 patients were genotyped successfully. Besides patients 1 and 2, no pathogenic mutation was detected. The CLCbio software showed that 96.24% and 93.6% of the data matched the reference sequences in patients 1 and 2, respectively. In the 357 targeted exons, 98.04% and 97.76% covered more than 10 reads. From patients 1 and 2, a total of 41 high-confidence variants were detected (table e-1 on the *Neurology*® Web site at www.neurology.org). In these variants, 39 known SNPs were coincident with the dbSNP or 1000 Genome database. Of the remaining 2 variants, the c.3248A>C in *KIF1A* was found in normal controls and was therefore considered as an SNP. A homozygous mutation in exon 22 of *SCN9A*, c. 3993delGinsTT, remained. This mutation was not observed in 100 Japanese control patient samples,

Figure 3 Pathologic findings from the sural nerve biopsies

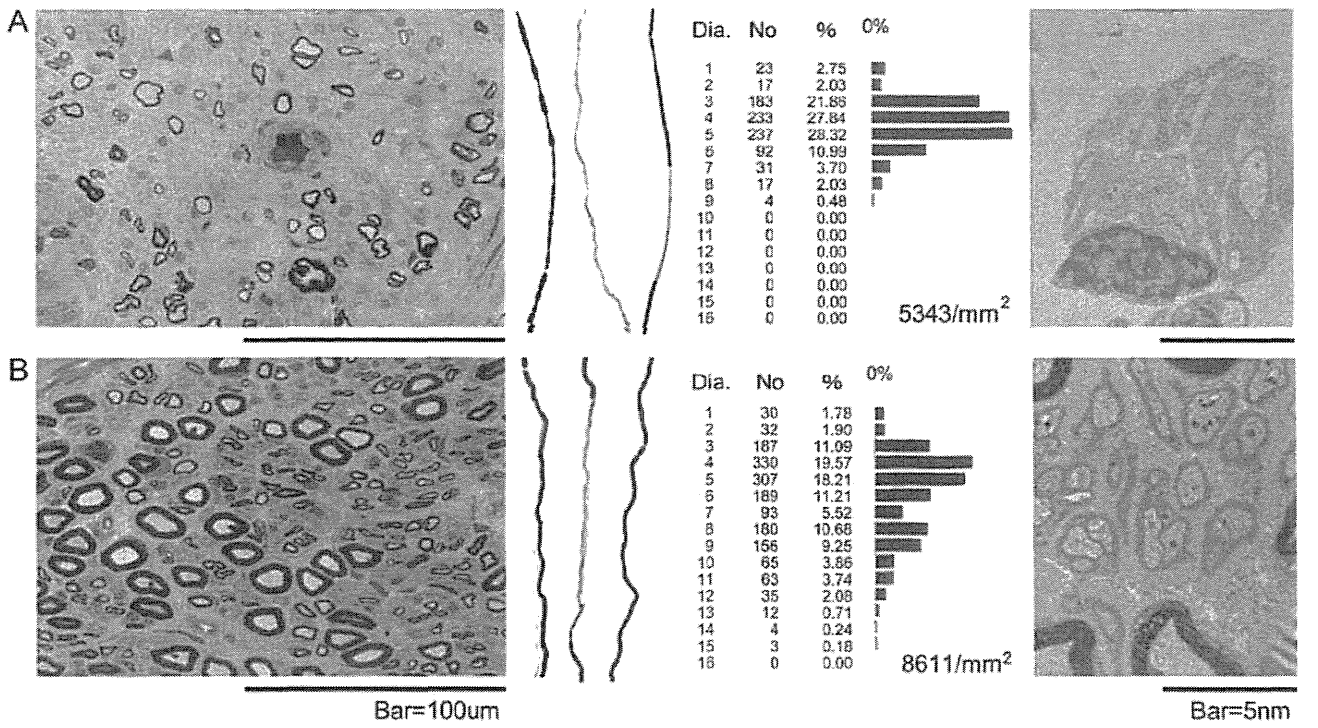

In patient 1, the density of large and small myelinated fibers is markedly decreased. The remaining myelinated fibers have thinner myelin sheaths. Some teased fibers exhibit axonal degeneration. The histogram of the fiber diameter indicates loss of large myelinated fibers (5,343 fibers/mm²). Electron microscopic examination shows clusters of Schwann cell processes (A). In patient 2, the densities of large and small myelinated fibers are slightly decreased. Teased fibers exhibit shortened internodal remyelination. The histogram of the fiber diameter shows a normal pattern (8,611 fibers/mm²). Unmyelinated fibers are fairly preserved, as shown under the electron microscope (B).

Figure 4 Pedigree diagram and genetic studies

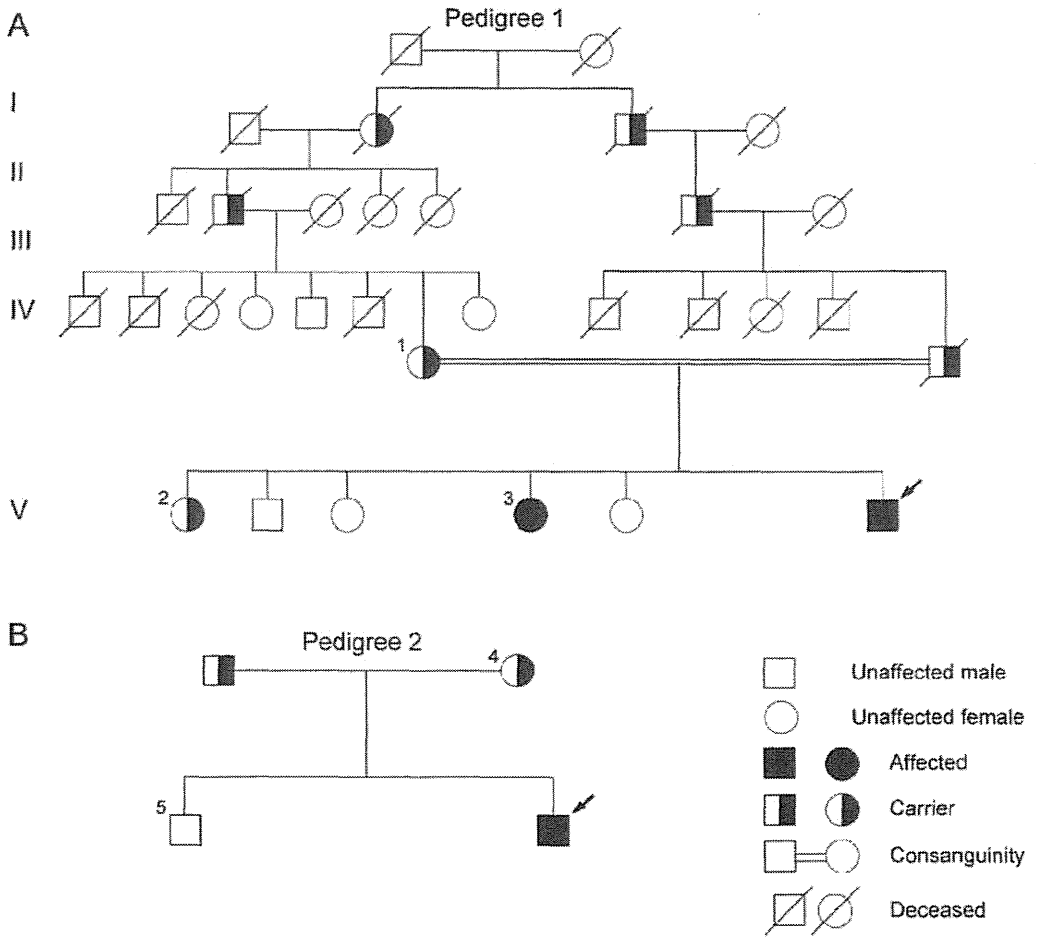

(A) Pedigree of patient 1. Patients 1 and 3 (V3) harbor the homozygous mutation, c.3993delGinsTT, whereas their mother (IV1) and 1 elder sister (V2) are heterozygous carriers. (B) Pedigree of patient 2. The same mutation, c.3993delGinsTT, can be observed in patient 2. His mother (4) exhibits the carrier genotype, and his elder brother (5) is normal. The black arrows (↙) indicate the proband. All the family members with available DNA samples are labeled with an Arabic numeral. (C) The c.3993delGinsTT mutation (↓) shifts the reading frame and generates a premature stop codon.

nor did we find it on the 1000 Genomes Web site, which catalogs human genetic variations using 2,500 patient samples, including 500 East Asian (100 Japanese) patient samples. DNA samples were then collected from 3 other family members of pedigree 1, and 2 members of pedigree 2. In patient 3, the same genotype was identified. In addition, asymptomatic carriers (mother and another elder sister of patient 1 and the mother of patient 2) and an unaffected member (brother of patient 2) were found (figure 4, A and B). This mutation changes the reading frame during the translation of the mRNA and generates a premature stop codon (figure 4C).

DISCUSSION Among the 16 disease-causing or related genes of HSAN, we identified a homozygous mutation in *SCN9A* from 2 Japanese families. We described 3 patients who presented with new clinical, in vivo electrophysiologic, and pathologic phenotypes.

SCN9A, which is located on chromosome 2q24.3, contains 26 coding exons.[32] It encodes $Na_v1.7$, which is the α-subunit of a tetrodotoxin-sensitive, voltage-gated sodium channel. $Na_v1.7$, composed of 4 domains, each with 6 transmembrane domains and 2 highly conserved pore-forming segments,[33] is preferentially expressed within the dorsal root ganglion and sympathetic ganglion neurons and their small-diameter peripheral

axons.[34] It is crucial for the depolarizing phase of neuronal action potentials, and it seems to determine the excitability and repetitive firing properties of neurons.[35] Gain-of-function *SCN9A* mutations result in hyperexcitable nociceptive neurons and states, such as inherited erythromelalgia,[18] paroxysmal extreme pain disorder,[19] and small nerve fiber neuropathy,[20] whereas loss-of-function *SCN9A* mutations produce no sodium current and generate CIP.[22]

In our study, both families lived in the Kagoshima prefecture, which is located to the south of Kyushu Island, Japan, and both were unrelated to each other. Loss of pain and temperature perceptions began at different ages, appearing as early as birth in patient 2, in the second decade in patient 1, and in the third decade in patient 3. Their ages at the onset of symptoms were different from those reported for patients with CIP who had a congenital onset. Moreover, in these 3 patients, the area of their pain insensitivities was limited mainly within the distal part of the limbs, not the entire body, as is seen in patients with CIP. The sense of vibration and joint position were preserved in our patients. However, the predominant reduction in sweat production in our 3 patients, together with urination and defecation disorder, lacrimal secretion anomaly, and decreased number of fungiform papilla on the tongue in patient 2, suggested autonomic nervous system dysfunction. A recent study indicated that $Na_v1.7$ in sympathetic neurons also contributes to the sensation of neuropathic pain.[36] The severe rash and pigmentation may be due to a post-inflammatory hyperpigmentation, resulting from the disruption of autonomic innervation. Meanwhile, hyposmia/anosmia, which is a common feature in patients with CIP and loss-of-functional *SCN9A* mutation,[23,27,37] was also identified in our patients. Furthermore, in patient 2, hypogeusia was detected using a gustatory sensation test. Bone dysplasia, as an additional symptom in patient 2 (acetabular dysplasia, short humerus, and right hallux), had also been reported in a Dutch kindred.[38] The otorhinolaryngologist confirmed hearing loss, although at different levels, in patients 1 and 2, which has mainly been recorded in patients with HSAN type IE.[4-6] These findings definitely broaden the symptomatic heterogeneity of *SCN9A* mutations.

Although pain insensitivity was symmetrically detected in the distal portion of the limbs of the 2 index patients, nerve conduction studies only revealed asymmetric involvement of the extremities. These findings, except those of the peroneal nerve, were compatible with sensory-predominant axonal multiple mononeuropathy complicated by minimal demyelinating changes, rather than a polyneuropathy.

Interestingly, the pathologic features of the sural nerve in the 2 index cases also varied. Although decreases in the small and large myelinated fibers were observed among the fasciculi in patient 1, the extent was dramatically different, whereas the density of small and large myelinated fibers was fairly preserved in patient 2. These discoveries were consistent with the nerve conduction study findings, which suggested a mismatch between the distribution of affected fibers and the severity of the loss-of-pain sensations. In addition, especially in patient 1, both decreased large myelinated fibers and decreased SNAP/SCV indicated that the large myelinated fibers were affected, whereas cases with gain-of-function *SCN9A* mutations always present with small myelinated and unmyelinated fiber abnormalities.[20] The selective involvement of sensory nerves in these patients is inconsistent with the clinical features and may indicate that the dysfunction of the dorsal root ganglion is more predominant than that of the peripheral nerve. However, the mechanisms underlying the pathologic aberrations in the fasciculi or nerves, caused by the mutated $Na_v1.7$ in the dorsal root ganglion, require further research.

The homozygous mutation, c.3993delGinsTT, which is located in exon 22 of *SCN9A*, is expected to shift the reading frame from amino acid 1331 (p. leu1331phe) and generate a premature stop codon. This will induce an essential alteration in the fifth transmembrane segment of domain 3 in $Na_v1.7$ and eliminate the whole fourth domain. The nonsense-mediated messenger RNA decay mechanism will then be activated, which will induce loss of function of $Na_v1.7$ in nociceptive neurons. Together with the pedigree study that confirmed the cosegregation of the genotype and phenotype, this mutation was believed to be a pathogenic mutation.

In 3 patients from 2 Japanese families who experienced symptoms that were characterized by congenital or adolescence-onset loss of pain and temperature perception and autonomic nervous dysfunction accompanied by hyposmia, hearing loss, hypogeusia, bone dysplasia, and fractures, we identified a novel loss-of-function frameshift *SCN9A* mutation. We demonstrated that this was a new entity on the basis of clinical, in vivo electrophysiologic, and pathologic findings. We introduce this new entity as HSAN type IID, an allelic disorder with CIP, both of which result from loss-of-function mutations in *SCN9A*. Furthermore, on the basis of in vivo electrophysiologic and pathologic findings, we furthered the understanding of the mechanisms induced by the loss of function of $Na_v1.7$. We are able to summarize that a loss-of-function *SCN9A* mutation can produce heterogeneous phenotype, even harboring the same mutation.

AUTHOR CONTRIBUTIONS

Dr. Junhui Yuan: genetic study, analyses and interpretation of data, and drafting the manuscript. Dr. Eiji Matsuura: pathologic study of the sural nerve, analysis and interpretation of data, revising the manuscript. Dr. Yujiro Higuchi: acquisition and analysis of clinical data, revising the manuscript. Dr. Akihiro Hashiguchi: acquisition of clinical data

and case selection. Dr. Tomonori Nakamura: nerve conduction study, analysis and interpretation of data. Dr. Satoshi Nozuma: acquisition of clinical data. Dr. Yusuke Sakiyama and Ms. Akiko Yoshimura: participated in genetic study. Dr. Shuji Izumo: analysis and interpretation of data. Dr. Hiroshi Takashima: study concept and design, interpretation of the data, revising the manuscript, study supervision, obtain funding.

ACKNOWLEDGMENT

The authors thank Ms. Y. Shirahama and A. Nishibeppu of our department for their excellent technical assistance. They also thank the Joint Research Laboratory, Kagoshima University Graduate School of Medical and Dental Sciences, for the use of their facilities.

STUDY FUNDING

Supported by the Intramural Research Grant (23-5) for Neurological and Psychiatric Disorders of NCNP; Research Committee for Neuropathy, Ataxic Disease and Applying Health and Technology of Ministry of Health, Welfare and Labour, Japan; and a research grant (23300201) from the Ministry of Health, Labour, and Welfare of Japan.

DISCLOSURE

Drs. Yuan, Matsuura, Higuchi, Hashiguchi, Nakamura, Nozuma, Sakiyama, and Ms. Yoshimura report no disclosures. Dr. Izumo received an honorarium for lecturing from Bayer Japan, funded by grants from Research Committee for HAM and neuroimmunological diseases of the Ministry of Health, Welfare and Labour of Japan. Dr. Takashima served on the scientific advisory board for Teijin, received a royalty from Athena diagnostics, was on the speakers' bureaus of Astellas, Bayer Group, Kyowa Hakko Kirin Pharma, Takeda Pharmaceutical Company Limited, Biogen Idec, Novartis, Dainippon Sumitomo Pharma, GlaxoSmithKline, Kowa Group, Pfizer Co., Mitsubishi Tanabe Pharma, and Eisai Co., is funded by grants from the Nervous and Mental Disorders and Research Committee for Ataxic Disease, Neuropathy, SMON, HAM, Chronic Pain, Applying Health and Technology of the Japanese Ministry of Health, Welfare and Labour, and received grants from Ministry of Education, Culture, Sports, Science, and Technology of Japan (grant 21591095). Go to Neurology.org for full disclosures.

Received November 2, 2012. Accepted in final form January 18, 2013.

REFERENCES

1. Dawkins JL, Hulme DJ, Brahmbhatt SB, Auer-Grumbach M, Nicholson GA. Mutations in SPTLC1, encoding serine palmitoyltransferase, long chain base subunit-1, cause hereditary sensory neuropathy type I. Nat Genet 2001;27:309–312.
2. Rotthier A, Auer-Grumbach M, Janssens K, et al. Mutations in the SPTLC2 subunit of serine palmitoyltransferase cause hereditary sensory and autonomic neuropathy type I. Am J Hum Genet 2010;87:513–522.
3. Guelly C, Zhu PP, Leonardis L, et al. Targeted high-throughput sequencing identifies mutations in atlastin-1 as a cause of hereditary sensory neuropathy type I. Am J Hum Genet 2011;88:99–105.
4. Wright A, Dyck PJ. Hereditary sensory neuropathy with sensorineural deafness and early-onset dementia. Neurology 1995;45:560–562.
5. Hojo K, Imamura T, Takanashi M, et al. Hereditary sensory neuropathy with deafness and dementia: a clinical and neuroimaging study. Eur J Neurol 1999;6:357–361.
6. Klein CJ, Botuyan MV, Wu Y, et al. Mutations in DNMT1 cause hereditary sensory neuropathy with dementia and hearing loss. Nat Genet 2011;43:595–600.
7. Lafreniere RG, MacDonald ML, Dube MP, et al. Identification of a novel gene (HSN2) causing hereditary sensory and autonomic neuropathy type II through the Study of Canadian Genetic Isolates. Am J Hum Genet 2004;74:1064–1073.
8. Coen K, Pareyson D, Auer-Grumbach M, et al. Novel mutations in the HSN2 gene causing hereditary sensory and autonomic neuropathy type II. Neurology 2006;66:748–751.
9. Kurth I, Pamminger T, Hennings JC, et al. Mutations in FAM134B, encoding a newly identified Golgi protein, cause severe sensory and autonomic neuropathy. Nat Genet 2009;41:1179–1181.
10. Rivière JB, Ramalingam S, Lavastre V, et al. KIF1A, an axonal transporter of synaptic vesicles, is mutated in hereditary sensory and autonomic neuropathy type 2. Am J Hum Genet 2011;89:219–230.
11. Slaugenhaupt SA, Blumenfeld A, Gill SP, et al. Tissue-specific expression of a splicing mutation in the IKBKAP gene causes familial dysautonomia. Am J Hum Genet 2001;68:598–605.
12. Anderson SL, Coli R, Daly IW, et al. Familial dysautonomia is caused by mutations of the IKAP gene. Am J Hum Genet 2001;68:753–758.
13. Axelrod FB, Hilz MJ. Inherited autonomic neuropathies. Semin Neurol 2003;23:381–390.
14. Mardy S, Miura Y, Endo F, et al. Congenital insensitivity to pain with anhidrosis: novel mutations in the TRKA (NTRK1) gene encoding a high-affinity receptor for nerve growth factor. Am J Hum Genet 1999;64:1570–1579.
15. Einarsdottir E, Carlsson A, Minde J, et al. A mutation in the nerve growth factor beta gene (NGFB) causes loss of pain perception. Hum Mol Genet 2004;13:799–805.
16. Carvalho OP, Thornton GK, Hertecant J, et al. A novel NGF mutation clarifies the molecular mechanism and extends the phenotypic spectrum of the HSAN5 neuropathy. J Med Genet 2011;48:131–135.
17. Edvardson S, Cinnamon Y, Jalas C, et al. Hereditary sensory autonomic neuropathy caused by a mutation in dystonin. Ann Neurol 2012;71:569–572.
18. Yang Y, Wang Y, Li S, et al. Mutations in SCN9A, encoding a sodium channel alpha subunit, in patients with primary erythermalgia. J Med Genet 2004;41:171–174.
19. Fertleman CR, Baker MD, Parker KA, et al. SCN9A mutations in paroxysmal extreme pain disorder: allelic variants underlie distinct channel defects and phenotypes. Neuron 2006;52:767–774.
20. Faber CG, Hoeijmakers JG, Ahn HS, et al. Gain of function Nav1.7 mutations in idiopathic small fiber neuropathy. Ann Neurol 2012;71:26–39.
21. Goldberg YP, Pimstone SN, Namdari R, et al. Human Mendelian pain disorders: a key to discovery and validation of novel analgesics. Clin Genet 2012;82:367–373.
22. Cox JJ, Reimann F, Nicholas AK, et al. An SCN9A channelopathy causes congenital inability to experience pain. Nature 2006;444:894–898.
23. Goldberg YP, MacFarlane J, MacDonald ML, et al. Loss-of-function mutations in the Nav1.7 gene underlie congenital indifference to pain in multiple human populations. Clin Genet 2007;71:311–319.
24. Ahmad S, Dahllund L, Eriksson AB, et al. A stop codon mutation in SCN9A causes lack of pain sensation. Hum Mol Genet 2007;16:2114–2121.
25. Cox JJ, Sheynin J, Shorer Z, et al. Congenital insensitivity to pain: novel SCN9A missense and in-frame deletion mutations. Hum Mutat 2010;31:e1670–e1686.
26. Staud R, Price DD, Janicke D, et al. Two novel mutations of SCN9A (Nav1.7) are associated with partial congenital insensitivity to pain. Eur J Pain 2011;15:223–230.

27. Nilsen KB, Nicholas AK, Woods CG, et al. Two novel SCN9A mutations causing insensitivity to pain. Pain 2009;143:155–158.
28. Schröder JM. Developmental and pathological changes at the node and paranode in human sural nerves. Microsc Res Tech 1996;34:422–435.
29. Dyck PJ, Giannini C, Lais A. Pathologic alterations of nerves. In: Dyck PJ, Thomas PK, Griffin JW, Low PA, Poduslo JF, editors. Peripheral Neuropathy, vol. 1, 3rd ed. Philadelphia: W.B. Saunders; 1993:514–595.
30. Milne I, Bayer M, Cardle L, et al. Tablet—next generation sequence assembly visualization. Bioinformatics 2010;26: 401–402.
31. Okamoto Y, Higuchi I, Sakiyama Y, et al. A new mitochondria-related disease showing myopathy with episodic hypercreatine kinase-emia. Ann Neurol 2011;70:486–492.
32. Michiels JJ, te Morsche RH, Jansen JB, Drenth JP. Autosomal dominant erythermalgia associated with a novel mutation in the voltage-gated sodium channel alpha subunit Nav1.7. Arch Neurol 2005;62:1587–1590.
33. Klugbauer N, Lacinova L, Flockerzi V, Hofmann F. Structure and functional expression of a new member of the tetrodotoxin-sensitive voltage-activated sodium channel family from human neuroendocrine cells. EMBO J 1995;14: 1084–1090.
34. Sangameswaran L, Fish LM, Koch BD, et al. A novel tetrodotoxin-sensitive, voltage-gated sodium channel expressed in rat and human dorsal root ganglia. J Biol Chem 1997;272:14805–14809.
35. Rush AM, Dib-Hajj SD, Liu S, Cummins TR, Black JA, Waxman SG. A single sodium channel mutation produces hyper- or hypoexcitability in different types of neurons. Proc Nad Acad Sci USA 2006;103:8245–8250.
36. Minett MS, Nassar MA, Clark AK, et al. Distinct Nav1. 7-dependent pain sensations require different sets of sensory and sympathetic neurons. Nat Commun 2012;3: 791.
37. Weiss J, Pyrski M, Jacobi E, et al. Loss-of-function mutations in sodium channel Nav1.7 cause anosmia. Nature 2011;472:186–190.
38. Hoeijmakers JG, Han C, Merkies IS, et al. Small nerve fibres, small hands and small feet: a new syndrome of pain, dysautonomia and acromesomelia in a kindred with a novel NaV1.7 mutation. Brain 2012;135:345–358.

Mitochondrial myopathy with autophagic vacuoles in patients with the m.8344A>G mutation

Jun-Hui Yuan, Yusuke Sakiyama, Itsuro Higuchi, Yukie Inamori, Yujiro Higuchi, Akihiro Hashiguchi, Keiko Higashi, Akiko Yoshimura, Hiroshi Takashima

▶ Additional material is published online only. To view please visit the journal online (http://dx.doi.org/10.1136/jclinpath-2012-201431).

Department of Neurology and Geriatrics, Kagoshima University, Graduate School of Medical and Dental Sciences, Kagoshima, Japan

Correspondence to
Dr Hiroshi Takashima, Department of Neurology and Geriatrics, Kagoshima University, Graduate School of Medical and Dental Sciences, 8-35-1 Sakuragaoka, Kagoshima City, Kagoshima 890-8520, Japan; thiroshi@m3.kufm.kagoshima-u.ac.jp

Received 28 December 2012
Accepted 11 March 2013 *
Published Online First 4 April 2013

ABSTRACT

Background and aims In mitochondrial myopathy, autophagy is presumed to play an important role in mitochondrial dysfunction. Rimmed vacuoles (RVs), a sign of autophagy, can be seen as a secondary phenomenon in muscle ragged-red fibres (RRFs), whereas the uncommon presentation is that some fibres contain RVs, but without any mitochondrial abnormalities. To investigate the pathogenesis beneath this pathological phenomenon.

Methods We reviewed 783 skeletal muscle specimens and selected five obtained from patients with suspected mitochondrial myopathy, characterised by clearly visible autophagic vacuoles in non-RRFs, besides the coexistence of RRFs and cytochrome oxidase-negative fibres. Immunohistochemical staining with LC-3, and electron microscopy studies were performed. Using resequencing microarray and a next-generation sequencing system, the mitochondrial DNA was screened for mutations and the heteroplasmic level was measured in skeletal muscle and blood.

Results Muscle fibres with RVs and RRFs, as well as some morphologically normal fibres, stained strongly for LC-3. Electron microscopy disclosed significant abnormal mitochondrial proliferation and existence of autophagic vacuoles. After mutation screening, m.8344A>G in the $tRNA^{Lys}$ gene was detected in two patients. The heteroplasmy of mutated G was 45.1% in skeletal muscle and 17.8% in blood in patient 1; patient 2 exhibited 80.3% mutated G in skeletal muscle and 25.2% in blood.

Conclusions These findings demonstrate a new pathological phenotype for the m.8344A>G mutation-related disease and also provide pathological evidence of a correlation between mitochondrial abnormalities and autophagy.

INTRODUCTION

Autophagy generally has a cytoprotective function, often preceding cellular apoptosis or necrosis. Cellular vacuoles that contain fragments of cell components are called autophagic vacuoles. Rimmed vacuoles (RVs) are characterised by small vacuoles lined by many red granules (the 'rim'), as observed by modified Gomori trichrome (mGT) staining and contain fragments of cellular components, including membrane whorls, as observed under electron microscopy. The RVs represent a type of autophagic vacuole and are non-disease-specific structures found in various myopathies, particularly in hereditary inclusion body myopathy, distal myopathy with RVs and inclusion body myositis (IBM).[1] Autophagy also contributes to the degradation of mitochondria (mitophagy),[2] and dysfunctional mitochondria may trigger the activation of the autophagic pathway.[3]

Ragged-red fibres (RRF) are characterised by the existence of subsarcolemmal zones of bright red or reddish blue material in mGT stain (figure 1), which result from the accumulation of abnormal mitochondria beneath the sarcolemma of muscle fibres. Histochemical demonstration of RRFs and cytochrome c oxidase-negative fibres on muscle biopsy is considered to be the hallmark of a mitochondrial myopathy.[4] In our experience, RVs can be seen in the RRFs, as a secondary change of abnormal mitochondrial accumulation. On the other hand, it has been shown that frequent RRFs can be found in patients with IBM and may reflect an age-related decline in muscle mitochondrial oxidative metabolism.[5] Nevertheless, in five Japanese patients with suspected mitochondrial myopathy, we found that besides the prominent feature of RRFs, noticeable RVs appeared in the non-RRFs—an unexpected phenomenon.

m.8344A>G mutation in the $tRNA^{Lys}$ gene can result in a myoclonic epilepsy with RRF (MERRF syndrome) and is present in over 80% of affected subjects. Genetic analysis showed an m.8344A>G mutation in two of our patients. Typical MERRF syndrome is characterised by myoclonic epilepsy, cerebellar ataxia and RRFs in skeletal muscle tissue.[6] However, in this study, the phenotypes of the two patients with the m.8344A>G mutation were atypical; they had proximal muscle weakness and external ophthalmoplegia or preferential facioscapulohumeral muscle involvement.

We demonstrate a new pathological phenotype for the m.8344A>G mutation. These findings suggest a distinct pathogenesis between mitochondrial abnormalities and autophagy. The isolated autophagic vacuoles may also be associated with the atypical clinical phenotype of patients with an m.8344A>G mutation.

MATERIALS AND METHODS

Subjects

We examined 783 skeletal muscle specimens obtained from patients who were referred to our department between 2001 and 2011. Twenty-seven patients with definite coexistence of RRFs and RVs were selected, and then those with IBM (10 patients), dermatomyositis (three patients), polymyositis (one patient), amyotrophic lateral sclerosis (two patients), myotonic dystrophy (one patient) and non-specific myopathy (five patients) were excluded. Based on the clinical features, marked RRFs and cytochrome c oxidase-negative fibres in pathology, five Japanese patients with suspected

To cite: Yuan J-H, Sakiyama Y, Higuchi I, *et al*. *J Clin Pathol* 2013;66: 659–664.

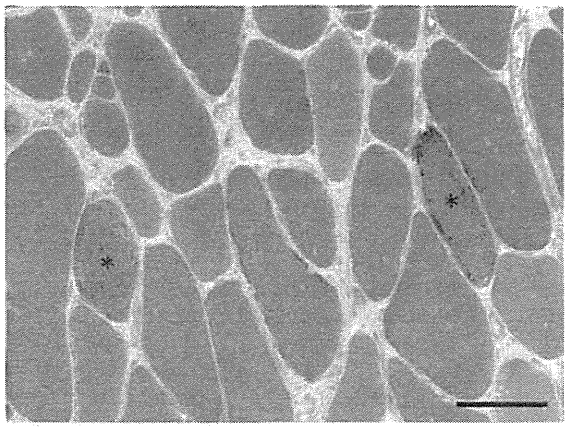

Figure 1 Modified Gomori trichrome staining of muscle ragged-red fibres (RRFs). RRFs are indicated by (*). Bar=100 μm. Access the article online to view this figure in colour.

mitochondrial myopathy were chosen for this study. Of these patients, only two who had the m.8344A>G mutation are described herein. No pathogenic mutation was detected in mtDNA from the other three patients. In addition, between 2001 and 2011, we identified the m.8344A>G mutation in blood from six of 169 patients with suspected mitochondrial disorders. Three of these patients underwent a muscle biopsy: two patients comprised the patients previously selected and the other exhibited a typical MERRF syndrome. However, because no definite RVs were seen in skeletal muscle, this last patient was excluded from the study.

All the diagnoses were made by experienced neurologists and pathologists based on clinical and laboratory examinations, electrobiological studies and skeletal muscle pathology.

Patient 1

A 51-year-old man with no family history of myopathy complained of general fatigue which he had had for 15 years. He began to experience muscle weakness from 36 years of age. This weakness gradually worsened, and by the age of 40 years he had difficulty in walking. Over the following 3 years, the symptoms progressed until he was incapable of lifting any substantial weight. Physical examination showed moderate muscle weakness in the facial, cervical and proximal muscles. His eye movements were also restricted in the superoinferior direction and he had difficulty hearing high-pitched voices. His serum creatine kinase level was raised at 1378 U/l (normal range 45–163 U/l).

Patient 2

A 54-year-old man reported a 24-year history of muscle weakness; there was no family history of any such difficulty. At 30 years of age, he experienced difficulty in lifting his arms and his cervical muscles gradually became affected. He occasionally tumbled down staircases; one fall required admission to hospital for a subarachnoid haemorrhage. Physical examination at the time of study enrolment showed marked weakness and wasting of the shoulder girdle muscles, without scapular winging. The facial muscles, intrinsic muscles of the hand and thigh muscles were also found to be atrophied. The extraocular muscles and the cranial nerves were normal and no other abnormalities were detected. His serum creatine kinase level was 46 U/l. CT indicated myoatrophy in his arms.

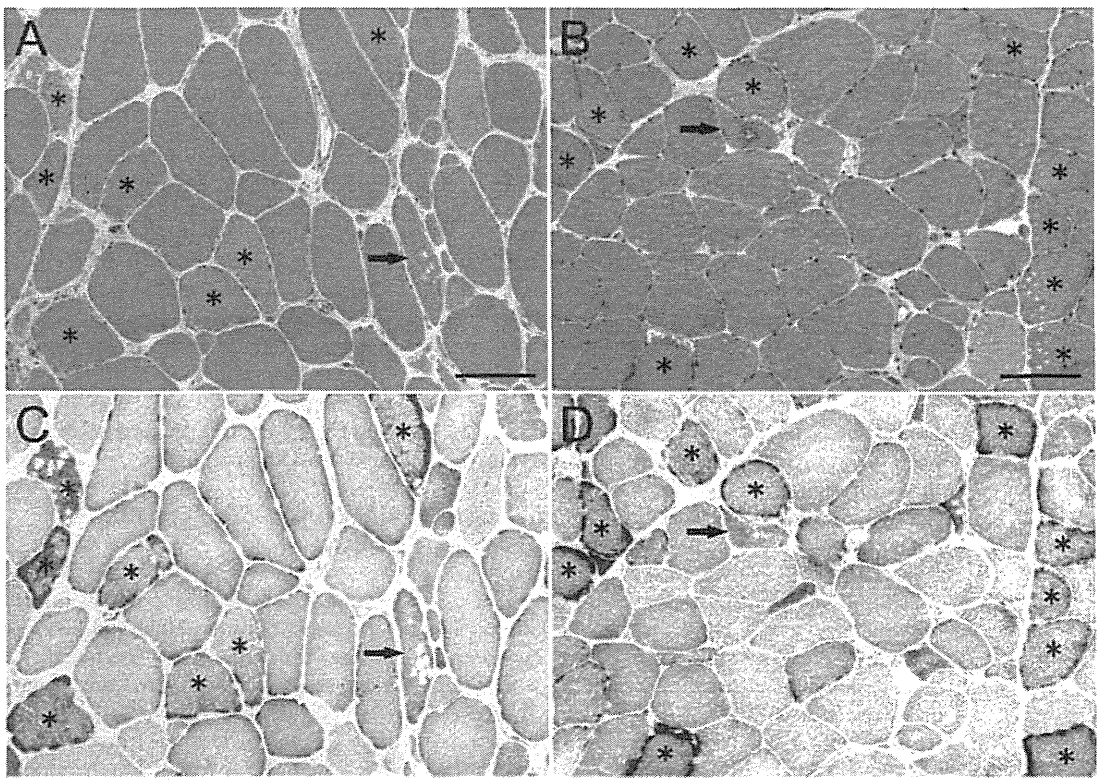

Figure 2 Histochemical staining of muscle ragged-red fibres (RRFs) and isolated rimmed vacuoles in patient 1 (A and C) and patient 2 (B and D). Haematoxylin and eosin (A and B) and succinate dehydrogenase (C and D) staining shows numerous RRFs (*), coexisting with non-RRFs containing rimmed vacuoles (arrow). Bar=100 μm. Access the article online to view this figure in colour.

We carried out a neurological examination and neuroradiological study in both patients and no comorbidities, including vascular disease, were seen, except for traumatic subarachnoid haemorrhage in patient 2.

Pathological studies

Skeletal muscle samples were obtained from the biceps brachii. Serial frozen sections (8 μm) were prepared and stained with multiple histochemical methods (see online supplementary table 1).

Other sections prepared on aminosilane-coated slides were immunohistochemically stained with 1:50 diluted microtubule-associated protein 1 light chain 3B (LC-3) clone 5F10 (Nano Tools, France). Biotinylated anti-mouse IgG was used as the secondary antibody and the avidin–biotin–peroxidase complex (ABC) method was used for signal detection (ABC kit; Vector Laboratories, Burlingame, California, USA). All the immunohistochemical procedures were performed as reported previously.[7]

A small amount of the muscle specimens was fixed in glutaraldehyde in cacodylate buffer, post-fixed in 1% buffered osmium tetroxide and then embedded in Epon. Semi-thin sections were prepared for light microscopy to localise the target region, while ultra-thin sections were cut and stained with uranyl acetate and lead citrate for electron microscopy. The electron microscopy procedures were performed as described previously.[8]

Mitochondrial DNA analysis

Genome DNA was extracted from both peripheral blood leucocytes (Qiagen, Maryland, USA) and frozen muscle specimens using a DNeasy blood and tissue kit (Qiagen). The entire mitochondrial DNA extracted from the skeletal muscles was sequenced using MitoChip V.2.0 (GeneChip Human Mitochondrial Resequencing Array 2.0) and analysed on GeneChip Sequence Analysis Software V.4.0.[9 10] Previously described primers were used,[11] and the variations detected by MitoChip V.2.0 were then confirmed by direct Sanger sequencing, as described.[12]

The polymorphic and pathogenic natures of the confirmed mutations were checked against two databases: MITOMAP (http://www.mitomap.org/) and GiiB-JST mtSNP (http://mtsnp.tmig.or.jp/mtsnp/index.shtml).

Heteroplasmic study

The GS Junior platform can sequence 1 00 000 single PCR fragments in parallel, which enables the detection of low levels of mtDNA heteroplasmy.[13 14] Using the Primer 3 program, we designed oligonucleotide primers flanking the m.8344A>G mutation (forward: 5′-CACTTTCACCGCTACACGAC-3′ and reverse: 5′-GCAATGAATGAAGCGAACAG-3′), which will generate a 428 bp PCR product. Using 50 ng genomic DNA from both blood and skeletal muscle of the two patients, after hot-start PCR, the products were sequenced on the GS Junior platform (Roche-454 Life Sciences, Basel, Switzerland) in accordance with the manufacturer's protocol. The results were assembled using the reference sequence (NC_012920) and analysed using GS Reference Mapper (454 Life Science) software.[15]

RESULTS

Pathological studies

In patients, histopathology showed moderate variation in muscle fibre size; numerous degenerating fibres with occasional regenerating or necrotic fibres were seen. RRFs were detected in 12.4% of muscle fibres (497/4001) in patient 1 and 20.7% of muscle fibres (253/1220) in patient 2. RVs were seen in occasional non-RRFs (figure 2). Cytochrome c oxidase activity was significantly decreased or absent in many fibres, particularly the RRFs, in which high succinate dehydrogenase expression was observed. The cytochrome c oxidase activity was increased in the non-RRF fibres containing isolated RVs. No blood vessels were seen that showed strong succinate dehydrogenase reactivity. Muscle fibres with RVs and RRFs, as well as some morphologically normal fibres, stained strongly for LC-3 (figure 3).

Electron microscopy in the biopsied muscle of the two patients disclosed significant abnormal mitochondrial proliferation with paracrystalline inclusions and circular arrangements of cristae. Autophagic vacuoles with membranous whorls and myelin-like structures were also seen (figure 4).

Mitochondrial DNA analysis

Using MitoChip V.2.0, 57 mitochondrial DNA variations were detected in skeletal muscle samples from the two patients and 54 were confirmed to be single nucleotide polymorphisms (SNPs) by referring to the MITOMAP and GiiB-JST mtSNP databases. An m.8344A>G mutation in the $tRNA^{Lys}$ gene was detected in both patients and subsequently confirmed by direct sequencing of DNA from both muscle and blood lymphocytes (figure 5). In addition, a new SNP, m.306C>A in the non-coding area and a missense mutation m.3433T>A (Tyr43Asp) in the ND1 gene of patient 2 were also found. However, considering the vital role of the $tRNA^{Lys}$ gene, we considered m.8344A>G to be the causative mutation.

Heteroplasmic study

Using the GS Junior platform, we clonally amplified and read more than 100 copies of each original amplicon from blood and muscle, in both patients. The percentage of 8344G in patient 1 was 17.8% (23/129) in blood and 45.1% (142/315) in muscle. In patient 2, the percentage was 25.2% (81/321) in blood and 80.3% (598/745) in muscle (figure 5).

DISCUSSION

We selected five patients with suspected mitochondrial myopathy and characterised by the coexistence of RRFs and isolated RVs in muscle fibres. Using a resequencing microarray and a next-generation sequencing system, we identified both the m.8344A>G mutation and its heteroplasmic nature in two of these patients.

m.8344A>G, with a prevalence rate of no more than 0.25/100 000 in Europe, is the most common mutation of MERRF syndrome.[16–18] The clinical variations of MERRF syndrome are extensively expanded to encephalitis, infantile putaminal necrosis, depression, Parkinson's disease, cardiomyopathy, neuropathy, ophthalmoplegia, chronic pancreatitis and the MELAS phenotype that comprises mitochondrial encephalomyopathy, lactic acidosis and stroke-like episodes.[19–26] In our study, patient 1 had progressive proximal muscle weakness, restriction of superoinferior eye movement and hearing loss. Patient 2 experienced isolated skeletal muscle effects, with involvement of the facial and proximal upper limb muscles. Although they harboured the MERRF mutation, both patients presented with nearly isolated myopathy rather than the typical MERRF syndrome with myoclonus epilepsy or cerebellar ataxia.

RRFs formed the predominant pathological feature in 12.4% and 20.7% of fibres in patients 1 and 2, respectively. The combination of cytochrome c oxidase-negative fibres and abnormally proliferated mitochondria found in electron microscopy, confirmed the pathological diagnosis of mitochondrial myopathy. In both patients haematoxylin and eosin and mGT staining

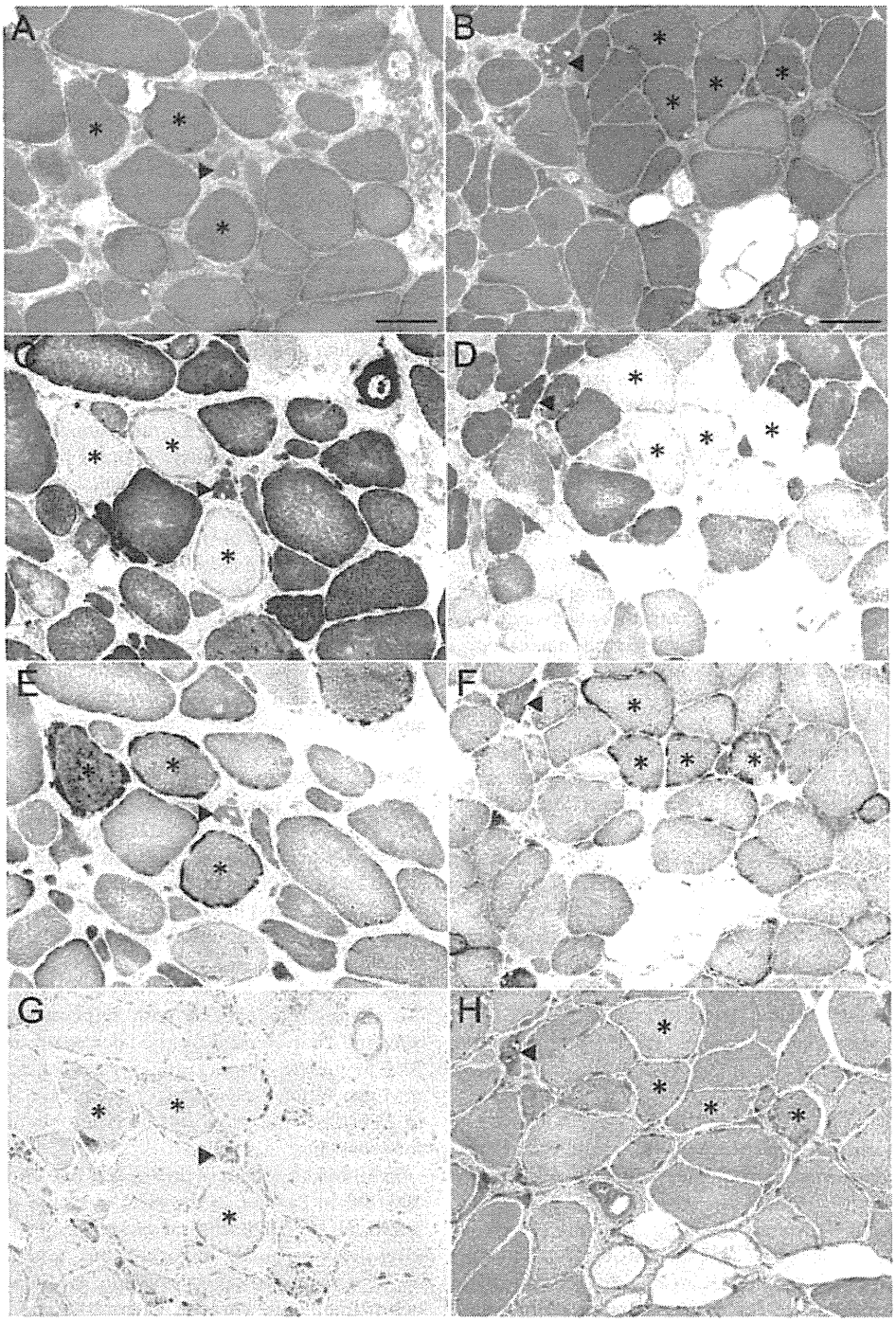

Figure 3 Serial sections of histochemical and immunohistochemical stained skeletal muscle samples in patient 1 (A, C, E and G) and patient 2 (B, D, F and H). Moderate myopathic change with coexistence of numerous in muscle ragged-red fibres (RRFs) (*) and some rimmed vacuoles (▲) is seen with the modified Gomori trichrome stain (A and B). Cytochrome c oxidase activity is significantly decreased or absent in many fibres, particularly RRFs (C and D), with high succinate dehydrogenase expression (E and F). Immunohistochemical staining of LC-3 was strong in fibres with rimmed vacuoles and RRFs and also in some morphologically normal fibres (G and H). Bar=100 μm. Access the article online to view this figure in colour.

demonstrated RVs in fibres without mitochondrial accumulation or loss of cytochrome c oxidase activity. LC-3 aggregation was seen in fibres with isolated RVs, RRFs with secondary vacuolation and even in some fibres without any morphological changes. These abnormalities suggest the overexpression of autophagy or disorders of autophagic pathways in these fibres.[27] Electron microscopy also confirmed the existence of autophagic vacuoles. Although mild autophagic changes can be seen in RRFs of patients with common mitochondrial myopathies, conspicuous RVs and LC3-positive fibres in non-RRFs were the characteristic findings in both of our study patients. Additionally, degeneration, regeneration or necrosis of muscle fibres indicated active cellular damage, probably resulting from mitochondrial dysfunction.

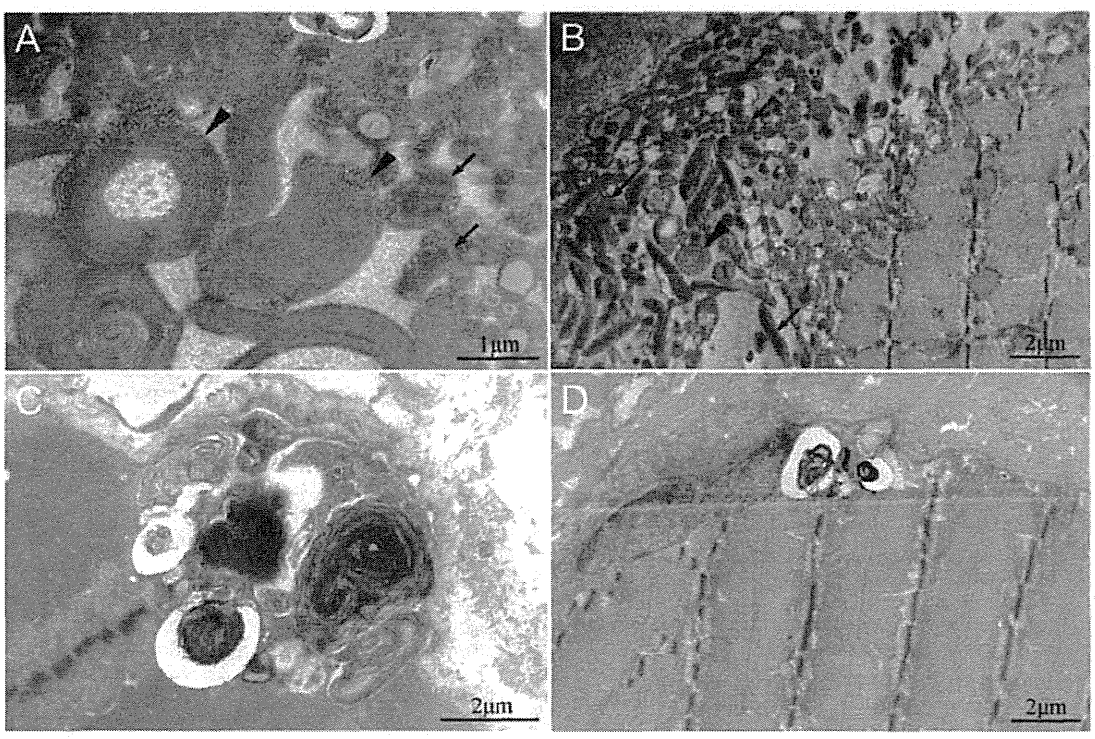

Figure 4 Electron microscopy of abnormal mitochondria and autophagic vacuoles in skeletal muscle tissue from patient 1 (A and C) and patient 2 (B and D). Significant abnormal mitochondrial proliferation is seen, with paracrystalline inclusions (↙) and circular arrangements of cristae (▲) (A and B). Some autophagic vacuoles have membranous whorls and myelin-like structures (C and D). Access the article online to view this figure in colour.

It has been reported that the $tRNA^{Lys}$ gene with the m.8344A>G mutation particularly lacks post-transcriptional modification of uridine at the first letter of the anticodon (the wobble position)[28]; mutant tRNAs without the wobble modification cannot fulfil their normal role as acceptor molecules in the translation process, which results in respiratory chain defects and also in impaired global protein synthesis and compromised mitochondrial translation products.[29 30] Cells with the m.8344A>G mutation were recently shown to have increased autophagic activity.[31] We therefore postulate that the singular devastating effect of the m.8344A>G mutation in the $tRNA^{Lys}$ gene is to induce active autophagy for the purpose of abnormal mitochondria removal.

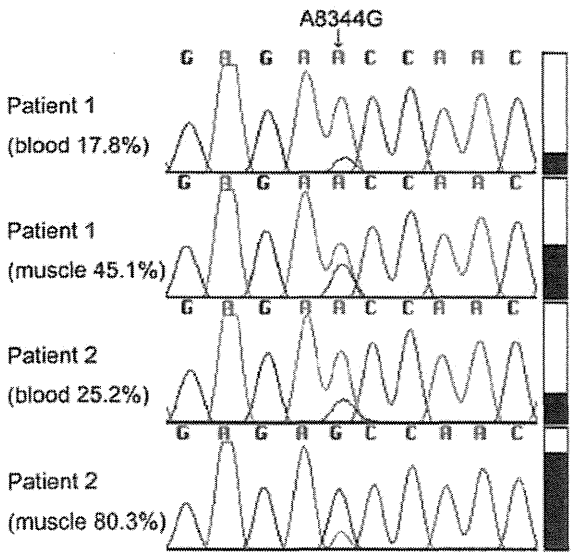

Figure 5 Sequence chromatograms and block diagrams of m.8344A>G mutation heteroplasmy in both blood and skeletal muscle DNA from the two patients. The mutation rate in blood and skeletal muscle was 17.8% and 45.1% in patient 1, respectively, and 25.2% and 80.3%, respectively, in patient 2. The arrow indicates the mutation site. Access the article online to view this figure in colour.

Mutations in mtDNA including m.8344A>G are always heteroplasmic, meaning that mutant and wild-type genomes coexist. The autophagic targeting of mitochondria adds to this heterogeneity.[32] The threshold for biochemical expression of a mtDNA mutation varies, depending on the mutation and the tissue involved. In the muscle fibres containing isolated RVs, the heteroplasmy of mutated G may be below the threshold required to cause a RRF, but trigger the autophagy pathway first. The GS Junior platform was used to confirm the heteroplasmy of 8344G, and the relatively low heteroplasmy level in blood may explain the predominantly skeletal muscle phenotype seen in the two patients. We recommend that patients suspected of having a mitochondrial disorder undergo genetic analysis of mtDNA, using muscle as the preferred tissue type.

In summary, we focused on a rare pathological phenomenon of coexistence of RRFs and isolated RVs, and identified the m.8344A>G mutation in two patients with atypical MERRF syndrome. This finding suggests that the distinctive pathogenesis results from the m.8344A>G mutation in both patients. The autophagy, always considered to be a secondary process after mitochondrial dysfunction, may work earlier than expected. Although the mechanism of detailed interaction between the m.8344A>G mutation and autophagy requires further investigation, these findings broaden the pathological phenotype of patients with the m.8344A>G mutation.

Take-home messages

- The interaction between autophagy and mitochondrial dysfunction remains unclear. The finding of isolated autophagic vacuoles in muscle fibres of patients with the m.8344A>G mutation, might be a starting point.
- The autophagic vacuoles, found in muscle fibres, might be associated with the atypical phenotype for a m.8344A>G mutation.
- The next-generation sequencing system might be reliable for detecting the heteroplasmy level of a mitochondrial DNA mutation.

Acknowledgements The authors thank N Hirata and Y Shirahama of our department for their excellent technical assistance. We also wish to thank the Joint Research Laboratory, Kagoshima University Graduate School of Medical and Dental Sciences for the use of their facilities.

Contributors J-HY carried out genetic experiments and drafted the manuscript. YS, YH and AY participated in genetic experiments and revised the manuscript. IH designed the study, revised the manuscript and obtained funding. YI, KH and AH carried out pathological and electron microscopy study. HT designed and supervised the study, revised the manuscript and obtained funding.

Funding The project was funded by the Ministry of Education, Culture, Sports, Science and Technology of Japan (grant 21591095 to HT; 21591094 to IH), intramural research grant (21B-1 to IH) for neurological and psychiatric disorders of the National Center of Neurology and Psychiatry, the Nervous and Mental Disorders and Research Committee for Charcot-Marie-Tooth disease, neuropathy, ataxic disease and applied health and technology of the Ministry of Health, Welfare and Labour, Japan and a research grant (23300201) from the Ministry of Health, Labour and Welfare of Japan.

Competing interests None.

Ethics approval Institutional review board of Kagoshima University.

Provenance and peer review Commissioned; externally peer reviewed.

REFERENCES

1 Kumamoto T, Ueyama H, Tsumura H, *et al*. Expression of lysosome-related proteins and genes in the skeletal muscles of inclusion body myositis. *Acta Neuropathol* 2004;107:59–65.
2 Kim I, Rodriguez-Enriquez S, Lemasters JJ. Selective degradation of mitochondria by mitophagy. *Arch Biochem Biophys* 2007;462:245–53.
3 Geisler S, Holmström KM, Skujat D, *et al*. PINK1/Parkin-mediated mitophagy is dependent on VDAC1 and p62/SQSTM1. *Nat Cell Biol* 2010;12:119–31.
4 DiMauro S, Hirano M, Kaufmann P, *et al*. Clinical features and genetics of myoclonic epilepsy with ragged red fibers. *Adv Neurol* 2002;89:217–29.
5 Rifai Z, Welle S, Kamp C, *et al*. Ragged red fibers in normal aging and inflammatory myopathy. *Ann Neurol* 1995;37:24–9.
6 Shoffner JM, Lott MT, Lezza AM, *et al*. Myoclonic epilepsy and ragged-red fiber disease (MERRF) is associated with a mitochondrial DNA tRNA(Lys) mutation. *Cell* 1990;61:931–7.
7 Higuchi I, Niiyama T, Uchida Y, *et al*. Multiple episodes of thrombosis in a patient with Becker muscular dystrophy with marked expression of utrophin on the muscle cell membrane. *Acta Neuropathol* 1999;98:313–16.
8 Niiyama T, Higuchi I, Suehara M, *et al*. Electron microscopic abnormalities of skeletal muscle in patients with collagen VI deficiency in Ullrich's disease. *Acta Neuropathol* 2002;104:67–71.
9 Zhou S, Kassauei K, Cutler DJ, *et al*. An oligonucleotide microarray for high-throughput sequencing of the mitochondrial genome. *J Mol Diagn* 2006;8:476–82.
10 Mithani SK, Smith IM, Zhou S, *et al*. Mitochondrial resequencing arrays detect tumor-specific mutations in salivary rinses of patients with head and neck cancer. *Clin Cancer Res* 2007;13:7335–40.
11 Rieder MJ, Taylor SL, Tobe VO, *et al*. Automating the identification of DNA variations using quality-based fluorescence re-sequencing: analysis of the human mitochondrial genome. *Nucleic Acids Res* 1998;26:967–73.
12 Sakiyama Y, Okamoto Y, Higuchi I, *et al*. A new phenotype of mitochondrial disease characterized by familial late-onset predominant axial myopathy and encephalopathy. *Acta Neuropathol* 2011;121:775–83.
13 Li M, Schönberg A, Schaefer M, *et al*. Detecting heteroplasmy from high-throughput sequencing of complete human mitochondrial DNA genomes. *Am J Hum Genet* 2010;87:237–49.
14 Tang S, Huang T. Characterization of mitochondrial DNA heteroplasmy using a parallel sequencing system. *Biotechniques* 2010;48:287–96.
15 Holland MM, McQuillan MR, O'Hanlon KA. Second generation sequencing allows for mtDNA mixture deconvolution and high resolution detection of heteroplasmy. *Croat Med J* 2011;52:299–313.
16 Chinnery PF, Johnson MA, Wardell TM, *et al*. The epidemiology of pathogenic mitochondrial DNA mutations. *Ann Neurol* 2000;48:188–93.
17 Darin N, Oldfors A, Moslemi AR, *et al*. The incidence of mitochondrial encephalomyopathies in childhood: clinical features and morphological, biochemical and DNA abnormalities. *Ann Neurol* 2001;49:377–83.
18 Remes AM, Majamaa-Voltti K, Kärppä M, *et al*. Prevalence of large-scale mitochondrial DNA deletions in an adult Finnish population. *Neurology* 2005;64:976–81.
19 Orcesi S, Gorni K, Termine C, *et al*. Bilateral putaminal necrosis associated with the mitochondrial DNA A8344G myoclonus epilepsy with ragged red fibers (MERRF) mutation: an infantile case. *J Child Neurol* 2006;21:79–82.
20 Molnar MJ, Perenyi J, Siska E, *et al*. The typical MERRF (A8344G) mutation of the mitochondrial DNA associated with depressive mood disorders. *J Neurol* 2009;256:264–5.
21 Horvath R, Kley RA, Lochmuller H, *et al*. Parkinson syndrome, neuropathy and myopathy caused by the mutation A8344G (MERRF) in tRNALys. *Neurology* 2007;68:56–8.
22 Vallance HD, Jeven G, Wallace DC, *et al*. A case of sporadic infantile histiocytoid cardiomyopathy caused by the A8344G (MERRF) mitochondrial DNA mutation. *Pediatr Cardiol* 2004;25:538–40.
23 Erol I, Alehan F, Horvath R, *et al*. Demyelinating disease of central and peripheral nervous systems associated with a A8344G mutation in tRNALys. *Neuromuscul Disord* 2009;19:275–8.
24 Naini AB, Lu J, Kaufmann P, *et al*. Novel mitochondrial DNA ND5 mutation in a patient with clinical features of MELAS and MERRF. *Arch Neurol* 2005;62:473–6.
25 Nishigaki Y, Tadesse S, Bonilla E, *et al*. A novel mitochondrial tRNA(Leu(UUR)) mutation in a patient with features of MERRF and Kearns-Sayre syndrome. *Neuromuscul Disord* 2003;13:334–40.
26 Toyono M, Nakano K, Kiuchi M, *et al*. A case of MERRF associated with chronic pancreatitis. *Neuromuscul Disord* 2001;11:300–4.
27 Kuma A, Matsui M, Mizushima N. LC3, an autophagosome marker, can be incorporated into protein aggregates independent of autophagy: caution in the interpretation of LC3 localization. *Autophagy* 2007;3:323–8.
28 Yasukawa T, Suzuki T, Ishii N, *et al*. Defect in modification at the anticodon wobble nucleotide of mitochondrial tRNA(Lys) with the MERRF encephalomyopathy pathogenic mutation. *FEBS Lett* 2000;467:175–8.
29 Masucci JP, Schon EA, King MP. Point mutations in the mitochondrial tRNA(Lys) gene: implications for pathogenesis and mechanism. *Mol Cell Biochem* 1997;174:215–19.
30 Yasukawa T, Suzuki T, Ishii N, *et al*. Wobble modification defect in tRNA disturbs codon-anticodon interaction in a mitochondrial disease. *EMBO J* 2001;20:4794–802.
31 Chen CY, Chen HF, Gi SJ, *et al*. Decreased heat shock protein 27 expression and altered autophagy in human cells harboring A8344G mitochondrial DNA mutation. *Mitochondrion* 2011;11:739–49.
32 Wikstrom JD, Twig G, Shirihai OS. What can mitochondrial heterogeneity tell us about mitochondrial dynamics and autophagy? *Int J Biochem Cell Biol* 2009;41:1914–27.

J Neurol
DOI 10.1007/s00415-012-6782-1

ORIGINAL COMMUNICATION

A family with IVIg-responsive Charcot–Marie–Tooth disease

Yasuo Miki · Masahiko Tomiyama · Rie Haga · Haruo Nishijima · Chieko Suzuki · Aiichiro Kurihara · Kazuhiro Sugimoto · Akihiro Hashiguchi · Hiroshi Takashima · Masayuki Baba

Received: 10 October 2012 / Revised: 26 November 2012 / Accepted: 29 November 2012

Abstract We report a family of intravenous immunoglobulin (IVIg)-responsive X-linked Charcot–Marie–Tooth disease Type 1 (CMT1X) with a novel gap junction protein 1 mutation. Two of three siblings in the family complained of subacute motor and sensory impairment, and their symptoms improved after the administration of IVIg. Additional IVIg treatment also resulted in similar improvement. The other also showed a mild improvement on IVIg. It has been suggested that an immune-mediated process is involved in the progression of neuropathy in CMT1X. The finding in our report provides evidence of susceptibility to immune-mediated demyelinating neuropathy in some form of CMT1X. Superimposed demyelinating neuropathy as well as a gradual deterioration of neuropathy over decades can be a clinical manifestation of CMT1X.

Y. Miki (✉) · M. Tomiyama · R. Haga · H. Nishijima · C. Suzuki · M. Baba
Department of Neurology, Aomori Prefectural Central Hospital, 2-1-1 Higashitsukurimichi, Aomori, Aomori 030-8553, Japan
e-mail: yasuomiki@hotmail.com

A. Kurihara
Department of Neurology, Aomori Rosai Hospital, Hachinohe, Aomori, Japan

K. Sugimoto
Diabetes Center, Ohta Nishinouchi Hospital, Koriyama, Fukushima, Japan

A. Hashiguchi · H. Takashima
Department of Neurology and Geriatrics, Kagoshima University Graduate School of Medical and Dental Sciences, Kagoshima, Kagoshima, Japan

Keywords X-linked Charcot–Marie–Tooth disease type 1 · Chronic inflammatory demyelinating polyneuropathy · IVIg · GJB1 · Immune-mediated demyelination

Introduction

Charcot–Marie–Tooth disease (CMT) encompasses a genetically heterogeneous group of hereditary motor and sensory neuropathies characterized by slowly progressive weakness and atrophy, primarily in the distal leg muscles. X-linked CMT type 1 (CMT1X) is the second most common type of CMT, which accounts for 7–10 % of all CMT. The prevalence of CMT1X is estimated to be between 1 in 25,000 and 1 in 35,000 [1]. The gene for the gap junction protein, beta 1, 32 kDa (http://www.genenames.org/data/hgnc_data.php?hgnc_id=4283) (*GJB1*) is designated to be causative for CMT1X [2]. A nerve conduction study (NCS) in male patients with CMT1X usually shows a uniform intermediate slowing of the motor nerve conduction velocity (MCV; 25–45 m/s) without a conduction block [3]. There is also a wide variability of clinical presentations and nerve involvement in CMT1X patients, even in those with the same missense mutation of the *GJB1* gene [4–6].

Chronic inflammatory demyelinating polyneuropathy (CIDP) is a clinically heterogeneous acquired polyneuropathy. CIDP evolves as a monophasic, relapsing, and progressive disorder that develops over a period of 8 weeks. The cause of CIDP is unknown and a single triggering antigen has yet to be determined.

Patients with CMT1X usually show a gradual deterioration in their symptoms. However, some patients with CMT1X experience a rapid progression of their motor or sensory symptoms and respond to immunotherapy,

Published online: 12 December 2012

including intravenous immunoglobulin (IVIg) [7–9]. These patients were diagnosed with coincidental CIDP and CMT.

We describe the clinical, electrophysiological, and genetic details of three affected offspring diagnosed with CMT1X and their mother. Two of three affected patients had a rapid aggravation of their symptoms, which were significantly alleviated with IVIg. The other also showed a mild improvement on IVIg. These findings indicate that CMT1X pathophysiology can trigger acquired demyelinating polyneuropathy, probably due to an immune-mediated process.

Case reports

The eldest brother

A 32-year-old male had trouble with sprinting due to drop foot in his early childhood. At the age of 28, he noticed rapidly progressing finger weakness and difficulty with fastening buttons. He also felt numbness of the bilateral soles and paresthesia of the distal extremities. At presentation, distal muscle weakness and atrophy were evident with a CMT disease neuropathy score (CMTNS) of 18 and a score of 20 for manual muscle testing (MMT) of ten selected muscles. All of the deep tendon reflexes were also absent. Cerebrospinal fluid (CSF) protein was slightly elevated at 44 mg/mL with a normal cell count. NCS revealed sensorimotor demyelinating polyneuropathy of all four limbs, with intermediate slowing of the MCV, temporal dispersion in the left median nerve, and A waves (Table 1). A sural nerve biopsy showed a significant reduction of large myelinated fibers with clusters of regenerating fibers. Onion bulbs and infiltration of inflammatory cells were not observed (Fig. 1). On the basis of his clinical presentation and intermediate low MCV, CMT1X was suspected, and a *GJB1* mutation was confirmed by a genetic test. However, the coincidental occurrence of acquired inflammatory neuropathy and CMT was also suspected based on the rapid deterioration of muscle weakness and sensory impairment, elevated CSF protein, and the NCS findings.

IVIg (0.4 g/kg for 5 days) was administered for the treatment of suspected acquired inflammatory neuropathy. His muscle weakness improved from 18 to 17 for the CMTNS, and the MMT score of ten selected muscles increased from 20 to 36. His sensory impairment was also alleviated. The effect of IVIg lasted only for 1 month. Three additional IVIg treatments showed a similar improvement each time. No significant improvement on NCS was seen during the course of the IVIg treatments. He has also improved on oral steroid therapy (30 mg/day) for 6 months.

The second-eldest brother

A 27-year-old male started to trip on stairs due to drop feet in his early childhood. It was not until 26 years old that he rapidly developed muscle weakness of the distal upper extremities and paresthesia of the fingers. At the age of 27, he visited a local orthopedic surgery because of his left hand paresthesia. Surgery for his left carpal-tunnel

Table 1 Nerve conduction studies of the patients

Location	Motor nerve				Sensory nerve	
	Distal latency (ms)	Amplitude (mV) distal/ proximal	Conduction velocity (m/s)	*F* wave	Amplitude (μV) distal/ proxymal	Conduction velocity (m/s)
The eldest brother						
Lt. median	4.9	1.2/0.4 (with TD)	33	A waves	3.6/0.9	35.7
Lt. ulnar	3.3	3.8/3.3	41.5	NE	4.9/4.2	31.3
Lt. tibial	6.7	0.2/0.2	33	NE		
Lt. sural					1.9	31
The second-eldest brother						
Lt. median	5	1.1/0.6	33.1	NE	1.7/NE	32.7
Lt. ulnar	3.8	2.0/1.6	37.1	A waves	7.2/NE	38.7
Lt. tibial	5.7	1.8/0.7	22.2	NE		
Lt. sural					2.9	32.9
The youngest sister						
Lt. median	5.5	1.0/0.9	30	NE	7.9/NE	33
Lt. ulnar	4.5	2.6/2.4	39	NE	4.9/NE	32
Lt. tibial	7.1	1.6/0.5	35	93.7		
Lt. sural					NE	NE

TD temporal dispersion, *NE* not evoked

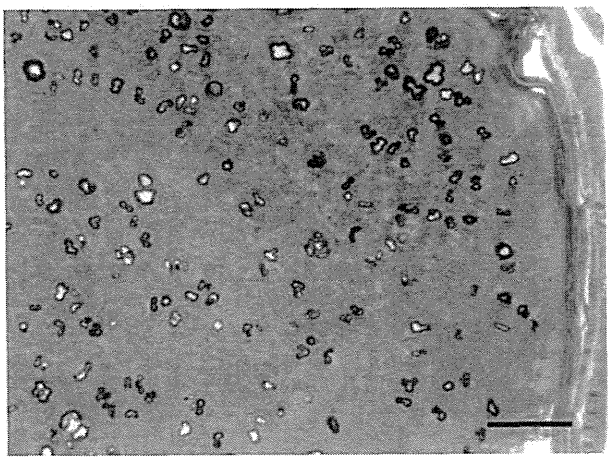

Fig. 1 The biopsied sural nerve of the eldest brother. A significant reduction of large myelinated fibers was observed with clusters of regenerating fibers. Formation of onion bulbs and infiltration of inflammatory cells were not seen. *Bar* = 50 μm

syndrome failed to alleviate the paresthesia. At presentation, a neurological examination revealed distal muscle weakness and atrophy of the limbs with an absence of all deep tendon reflexes and decreased vibration perception of the bilateral lower extremities. The patient had a CMTNS of 12 and an MMT score of 34 for ten selected muscles. An NCS showed sensorimotor demyelinating polyneuropathy with a non-uniform slowing of the MCV. Furthermore, variability of the MCV among nerves was also evident (Table 1). The outcome of a genetic test showed the same *GJB1* mutation as his elder brother.

Due to the acute emergence of his left hand paresthesia and NCS findings, he was also suspect of having acquired inflammatory neuropathy superimposed on CMT1X. The patient was treated with IVIg, resulting in an improvement of his muscle weakness, while his MMT score and CMTNS changed from 34 to 42 and from 12 to 11, respectively. An NCS showed no significant change after IVIg treatment.

The youngest sister

A 24-year-old female visited our outpatient clinic in order to have a genetic examination. At the age of 7, she had difficulty in uncorking a bottle. She never felt a stepwise deterioration. At the first visit, she could not perform dorsiflexion of her toes, but distal muscle weakness of her limbs was mild and graded as MMT 4 or 4+. Her CMTNS and MMT score of ten selected muscles were 10 and 44, respectively. An NCS demonstrated diffuse sensorimotor demyelinating polyneuropathy (Table 1). We confirmed that she had the same *GJB1* mutation as her brothers.

After the administration of IVIg, only extension of her large toes was observed.

Mother of the three patients

She complained of no clinical symptoms and her NCS findings were normal. We confirmed that she had the same GJB1 mutation as her children.

Mutation screening

After written informed consent was given from all family members, we screened for mutations in all *GJB1* coding exons in comparison to the published sequence (NM_000166) using the standard Sanger method. We also screened for duplication of the peripheral myelin protein 22 (*PMP22*) gene using fluorescent in situ hybridization (FISH).

Mutation analysis of *GJB1* in this family and a control study

From the family history and clinical information, we screened for mutations in the *GJB1* gene and detected a novel c.227T > G (p.L76R) missense mutation. In contrast, analysis using an original gene chip was negative for mutations involving the other 27 CMT genes or related disease-causing genes [10]. The patients do not have a *PMP22* duplication as determined by FISH.

The eldest brother was hemizygous for the c.227T > G mutation, which substitutes a leucine for arginine at amino acid 76 (p.L76R) in exon 2 of *GJB1* according to conceptual translation (Fig. 2). The younger brother had the same hemizygous mutation, and his mother and sister were heterozygous for this mutation (Fig. 2). We did not observe p.L76R in 112 controls or in 446 patients with inherited neuropathy. In addition, we did not find the p.L76R mutation in the 1000 Genomes website (http://browser.1000genomes.org), which catalogs human genetic variations using 1,197 samples, including 300 East Asian (100 Japanese) samples. Family segregation studies suggest that it is reasonable to assume that the L76R mutation was the cause of CMT in this family.

Discussion

Since Dyck's first report of seven prednisone-responsive CMT patients with stepwise deteriorating neuropathy, it has long been recognized that rapid progression and non-uniform demyelination with a conduction block or temporal dispersion could also occur in some patients with CMT. These patients responded to immunotherapy, including corticosteroids or IVIg [7, 11]. In fact, some patients with CMT1X are erroneously diagnosed as CIDP when an NCS shows non-uniform nerve conduction [12].

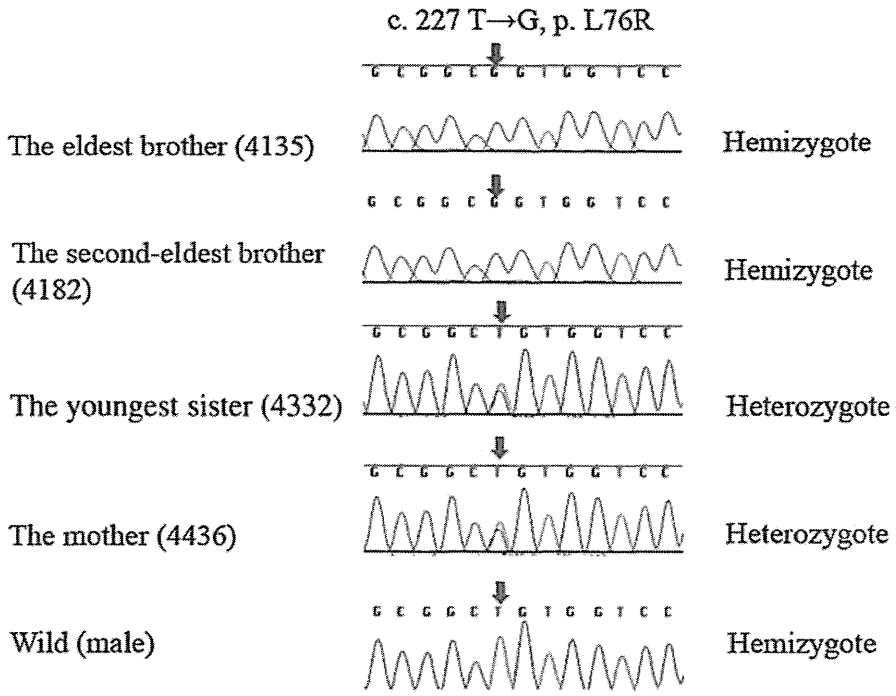

Fig. 2 *GJB1* alterations identified in the family. Chromatograms of the alterations in the *GJB1* gene. A hemizygous mutation was identified in the eldest brother (4135) and second-eldest brother (4182). A heterozygous mutation was identified in the youngest sister (4332) and mother (4436). The transition c.227T > G resulted in p.L76R

There have been three reports in which all of the CMT1X patients experienced a stepwise deterioration in neuropathy and responded to IVIg [4, 5, 9]. Thus, the superimposition of neuropathy and CMT was thought to be linked by some common mechanism. The condition is, however, reported as the coincidental occurrence of CIDP and CMT because the number of previous reports is limited, and there is only one report describing the occurrence of acquired inflammatory polyneuropathy along with the gradual deterioration of CMT1X in a single family [9].

The two brothers in our report showed stepwise deterioration after periods of clinical stability. Their symptoms showed a significant improvement with IVIg therapy. Repetitive IVIg relieved the stepwise deterioration in the eldest brother; furthermore, a mild motor improvement was also seen in the sister without any sign of neuropathy mimicking CIDP. Of particular note is that all of the affected siblings diagnosed with CMT1X responded to IVIg. It seems stochastically unlikely that two out of three family members with CMT1X, with a prevalence of 1 in 35,000, experienced CIDP, with a prevalence of 1 in 100,000 [13]. These findings provide strong evidence that patients with CMT1X might be susceptible to IVIg-responsive demyelination during the course of CMT1X. NCS did not show any conduction blocks and improvement of the temporal dispersion in the eldest brother after IVIg treatment in examined nerves of the affected siblings. We speculate that conduction blocks might have existed and been improved in more distal nerves after IVIg administration.

How immunoregulation by steroids and IVIg alleviates the stepwise deterioration in patients with CMT1X remains to be elucidated. Evidence from animal models of CMT1X, however, suggests that an immune-mediated process is involved in the progression of neuropathy in CMT1X. In the gap junction component connexin32 deficient mice, numerous macrophages are found in the peripheral nerves before a migration of T cells. Once the macrophages become activated, they attract T cells. CD8-positive T cells presented with antigens, possibly of myelin origin, cause further activation of macrophages [14]. Kobsar et al. [15] showed that cross-bred connexin32-deficient mice with recombination activating gene-1-deficient mice, which lack mature T- and B-lymphocytes, showed a significant reduction of demyelinated peripheral nerves. Recently, a null mice mutant for colony-stimulating factor, a pivotal macrophage activator, demonstrated significant amelioration of demyelination [16]. Although no infiltration of inflammatory cells was seen in the left sural nerve biopsy of the eldest brother in the present study, the *GJB1* mutation might have resulted in a predisposition to develop immune-mediated demyelinating polyneuropathy in addition to the underlining CMT1X pathology, potentially as the result of the activation of macrophages. IVIg might have beneficial immunomodulating effects on stepwise deterioration of neuropathy in our patients.

In this study, we clearly demonstrated a family of IVIg-responsive patients with CMT1X. Immune-mediated demyelination can be partially responsible for the pathogenesis of CMT1X, not merely the coincidental occurrence

of CIDP with CMT. Some patients with CMT1X can experience rapid deterioration due to immune-mediated demyelination along with a steady decline in their symptoms. Both stepwise and gradual deterioration can be clinical manifestations of CMT1X.

Acknowledgments We thank the family described in this report for their cooperation. We also thank Ms. A. Yoshimura of Kagoshima University for her excellent technical assistance. This study was supported in part by grants from the Nervous and Mental Disorders and Research Committee for Charcot–Marie–Tooth Disease, Neuropathy, Ataxic Disease, and Research on Applying Health Technology of the Japanese Ministry of Health, Welfare, and Labor (H.T.).

Conflicts of interest We declare no conflict of interest.

Ethical standard This study was conducted with the approval of the Aomori Prefectural Central Hospital ethical committee.

References

1. Pareyson D, Marchesi C (2009) Diagnosis, natural history, and management of Charcot–Marie–Tooth disease. Lancet Neurol 8:654–667
2. Bergoffen J, Scherer SS, Wang S et al (1993) Connexin mutations in X-linked Charcot–Marie–Tooth disease. Science 262:2039–2042
3. Hattori N, Yamamoto M, Yoshihara T et al (2003) Demyelinating and axonal features of Charcot–Marie–Tooth disease with mutations of myelin-related proteins (PMP22, MPZ and Cx32): a clinicopathological study of 205 Japanese patients. Brain 126: 134–151
4. Gutierrez A, England JD, Sumner AJ et al (2000) Unusual electrophysiological findings in X-linked dominant Charcot–Marie–Tooth disease. Muscle Nerve 23:182–188
5. Kuntzer T, Dunand M, Schorderet DF et al (2003) Phenotypic expression of a Pro 87 to Leu mutation in the connexin 32 gene in a large Swiss family with Charcot–Marie–Tooth neuropathy. J Neurol Sci 207:77–86
6. Tabaraud F, Lagrange E, Sindou P et al (1999) Demyelinating X-linked Charcot–Marie–Tooth disease: unusual electrophysiological findings. Muscle Nerve 22:1442–1447
7. Ginsberg L, Malik O, Kenton AR et al (2004) Coexistent hereditary and inflammatory neuropathy. Brain 127:193–202
8. Ryan MM, Jones HR Jr (2005) CMTX mimicking childhood chronic inflammatory demyelinating neuropathy with tremor. Muscle Nerve 31:528–530
9. Sakaguchi H, Yamashita S, Miura A et al (2001) A novel GJB1 frameshift mutation produces a transient CNS symptom of X-linked Charcot–Marie–Tooth disease. J Neurol 258:284–290
10. Nakamura T, Hashiguchi A, Suzuki S et al (2012) Vincristine exacerbates asymptomatic Charcot–Marie–Tooth disease with a novel EGR2 mutation. Neurogenetics 13:77–82
11. Dyck PJ, Swanson CJ, Low PA et al (1982) Prednisone-responsive hereditary motor and sensory neuropathy. Mayo Clin Proc 57:239–246
12. Michell AW, Laura M, Blake J et al (2009) GJB1 gene mutations in suspected inflammatory demyelinating neuropathies not responding to treatment. J Neurol Neurosurg Psychiatry 80:699–700
13. Lunn MP, Manji H, Choudhary PP et al (1999) Chronic inflammatory demyelinating polyradiculoneuropathy: a prevalence study in south east England. J Neurol Neurosurg Psychiatry 66:677–680
14. Martini R, Toyka KV (2004) Immune-mediated components of hereditary demyelinating neuropathies: lessons from animal models and patients. Lancet Neurol 3:457–465
15. Kobsar I, Berghoff M, Samsam M et al (2003) Preserved myelin integrity and reduced axonopathy in connexin32-deficient mice lacking the recombination activating gene-1. Brain 126:804–813
16. Groh J, Weis J, Zieger H et al (2012) Colony-stimulating factor-1 mediates macrophage-related neural damage in a model for Charcot–Marie–Tooth disease type 1X. Brain 135:88–104

特集　神経疾患をもつ患者の妊娠・出産

HTLV-1関連脊髄症(HAM)と妊娠・出産*

松崎敏男**,***／出雲周二**

Key Words：HTLV-1, mother to child transmission, breast milk, high HTLV-1 provirus load

はじめに

HTLV-1関連脊髄症(HAM)は慢性に進行する両下肢痙性麻痺と排尿排便障害，感覚障害を呈する難治性疾患で[1][2]，2008年(平成20年)から厚生労働省の難治性疾患克服研究事業の調査研究対象疾患になっている．近年行われた疫学調査[3]では，有病率は人口10万人あたり約3人，全国で3,000人あまりの患者がいると推定されている．HTLV-1キャリアの動向[4]と連動して，西南日本に多いものの九州で減少傾向，関東・近畿の大都市圏では増加傾向を示し，全国どこでもHAM患者の診療機会があるものと考えられる．また，発症年齢の高齢化が示されているが，20歳代，30歳代の若年発症者も少なからずみられ，男女比が1：2～2.5と女性に多いために今回のテーマである妊娠・出産にかかわることも稀ではないと思われる．本稿では，妊娠前後よりHAMの臨床症状があり，妊娠・出産後の経過を追えた自験例を紹介し，HAMにおける妊娠・出産の影響について考察したい．

自験例の紹介

〔症例1〕50歳，女性．

家族歴：なし．

既往歴：5歳リウマチ熱，20歳虫垂炎手術．

現病歴：23歳時，第1子出産．第1子の妊娠・出産で問題なく，HAMを示唆する症状もなかった．24歳時，第2子妊娠時より日中約10回の頻尿傾向であり，妊娠経過は順調で正常分娩で出産した．出産後も頻尿の改善はなかった．靴の外側がすれ，両膝以下のしびれ感と下肢のつっぱりが出現し，26歳時に泌尿器科を経て内科から神経内科に紹介され，HAMと診断された．両下肢軽度筋力低下と痙性歩行，四肢深部反射亢進，両側Babinski反射・Chaddock反射陽性，両膝下異常知覚，感覚低下，内反尖足，Th10以下発汗低下，1日頻尿14回，便秘を認め，運動機能障害は2/13段階で走れないが，階段で手すりは使用しない状態であった．血清髄液抗HTLV-1抗体陽性，髄液細胞数27/3と軽度増加していた．シストメトリーで尿道括約筋協調不全．エリスロマイシン600mgの内服により頻尿の改善がみられている．29歳時，末梢血HTLV-1プロウイルス量922コピー/10^4末梢血リンパ球(PBMC)であった．41歳時，運動機能は変わらず，48歳時に痙性歩行悪化で一本杖となったが，ステロイド内服療法をうけ，現在は杖なしで歩行可能となっている．

〔症例2〕35歳，女性．

家族歴・既往歴：特記することはない．輸血

* Pregnancy and delivery with HTLV-1-associated myelopathy.
** Toshio MATSUZAKI, M.D. & Shuji IZUMO, M.D.: 鹿児島大学大学院医歯学総合研究科附属難治ウイルス病態制御研究センター分子病理病態研究分野〔〒890-8544　鹿児島県鹿児島市桜ヶ丘8-35-1〕; Division of Molecular Pathology, Center for Chronic Viral Diseases, Kagoshima University, Kagoshima 890-8544, Japan.
*** 兼　大勝病院神経内科; Department of Neurology, Okatsu Hospital, Kagoshima, Japan.